Chaos analysis of viscoelastic chaotic flows of polymeric fluids in a micro-channel

Han, J.; Lim, Chun Ping; Lam, Yee Cheong

2015

Lim, C. P., Han, J., & Lam, Y. C. (2015). Chaos analysis of viscoelastic chaotic flows of polymeric fluids in a micro-channel. AIP Advances, 5, 077150-.

https://hdl.handle.net/10356/79307

https://doi.org/10.1063/1.4927474

AIP Advances

Chaos analysis of viscoelastic chaotic flows of polymeric fluids in a micro-channel

C. P. Lim, J. Han, and Y. C. Lam

Citation: AIP Advances **5**, 077150 (2015); doi: 10.1063/1.4927474
View online: http://dx.doi.org/10.1063/1.4927474
View Table of Contents: http://scitation.aip.org/content/aip/journal/adva/5/7?ver=pdfcov
Published by the AIP Publishing

Chaos analysis of viscoelastic chaotic flows of polymeric fluids in a micro-channel

C. P. Lim,[1,2] J. Han,[2,3,4] and Y. C. Lam[1,2,a]
[1]*School of Mechanical and Aerospace Engineering, Nanyang Technological University, 639798, Singapore*
[2]*BioSystems and Micromechanics (BioSyM) IRG, Singapore-MIT Alliance for Research and Technology (SMART) Centre, 138602, Singapore*
[3]*Department of Electrical Engineering and Computer Science, Massachusetts Institute of Technology, Cambridge, MA 02139, USA*
[4]*Department of Biological Engineering, Massachusetts Institute of Technology, Cambridge, MA 02139, USA*

(Received 17 April 2015; accepted 15 July 2015; published online 22 July 2015)

Many fluids, including biological fluids such as mucus and blood, are viscoelastic. Through the introduction of chaotic flows in a micro-channel and the construction of maps of characteristic chaos parameters, differences in viscoelastic properties of these fluids can be measured. This is demonstrated by creating viscoelastic chaotic flows induced in an H-shaped micro-channel through the steady infusion of a polymeric fluid of polyethylene oxide (PEO) and another immiscible fluid (silicone oil). A protocol for chaos analysis was established and demonstrated for the analysis of the chaotic flows generated by two polymeric fluids of different molecular weight but with similar relaxation times. The flows were shown to be chaotic through the computation of their correlation dimension (D_2) and the largest Lyapunov exponent (λ_1), with D_2 being fractional and λ_1 being positive. Contour maps of D_2 and λ_1 of the respective fluids in the operating space, which is defined by the combination of polymeric fluids and silicone oil flow rates, were constructed to represent the characteristic of the chaotic flows generated. It was observed that, albeit being similar, the fluids have generally distinct characteristic maps with some similar trends. The differences in the D_2 and λ_1 maps are indicative of the difference in the molecular weight of the polymers in the fluids because the driving force of the viscoelastic chaotic flows is of molecular origin. This approach in constructing the characteristic maps of chaos parameters can be employed as a diagnostic tool for biological fluids and, more generally, chaotic signals. [http://dx.doi.org/10.1063/1.4927474]

Fluid flows in microfluidic channels are often laminar and not chaotic due to the low Reynolds' number (Re) for flows in micro-scale dimensions, i.e. negligible inertial forces. Nonetheless, non-inertia driven chaotic flows can be induced in micro-channels by other forces such as acoustic forces,[1] interfacial tension[2,3] and viscoelastic forces.[4–6] With the addition of a trace amount of polymers, a fluid becomes viscoelastic, exhibiting both viscous and elastic characteristics. Chaotic flows of viscoelastic, polymeric fluids were demonstrated in a micro-channel by exploiting their non-linear behavior through the introduction of curved streamlines[4] and sudden changes in geometry.[6] Viscoelastic chaotic flows are deterministic but not easily predictable; this is the hallmark of chaos, in the sense that minute differences in initial conditions would lead to significantly different flow states. Characterization of these non-linear complex flows requires chaos analysis.

[a]Author to whom correspondence should be addressed. Electronic mail: myclam@ntu.edu.sg.

Through chaos analysis, chaotic flows can be characterized by their chaos parameters such as the largest Lyapunov exponent (λ_1), the correlation dimension (D_2), the correlation entropy (K_2), *etc*.[7] Chaos analysis was previously employed in flow regime identification of two phase flows in horizontal pipe,[8] in T-junction[9] and in bubble column.[10,11] The onset of chaos in a mixing process[12] and chaotic advection of particles[13] could also be determined by such analysis. In this investigation, viscoelastic chaotic flows of polymeric fluids were generated in a micro-channel. The chaotic flows were characterized by D_2 (fractional D_2 indicates chaos) and λ_1 (positive λ_1 indicates chaos). D_2 represents the complexity of a chaotic flow while λ_1 its unpredictability. These two parameters can be described by maps that portray the differences in the chaos generated by systems with close similarity.

By their very nature, many fluids, including biological fluids such as mucus and blood, are viscoelastic. Conventional rheological measurements measure the bulk rheological properties of different fluids but are not adequate in capturing all their (non-linear) viscoelastic properties, often originating from molecular level differences. In this paper, we propose a novel characterization method of viscoelastic fluids by inducing chaotic flows in a micro-channel and the construction of characteristic chaos parameter maps. This method can potentially be employed as a diagnostic tool for biological fluids such as mucus and blood, potentially revealing subtle differences that are not clearly discernible by bulk rheological parameters (e.g. viscosity). In addition, this analysis can bring new paradigm to the analysis of chaotic signals such as electrocardiograms[14] and signals from fetal heart rate monitoring techniques.[15]

Viscoelastic chaotic flows of two polymeric fluids were generated in an H-shaped micro-channel (H-micro-channel) as shown in Fig. 1(a). It has a Center Channel (CC) with the width of 50μm, and two main channels, *i.e.* Main Channel 1 (MC 1) and Main Channel 2 (MC 2) with the

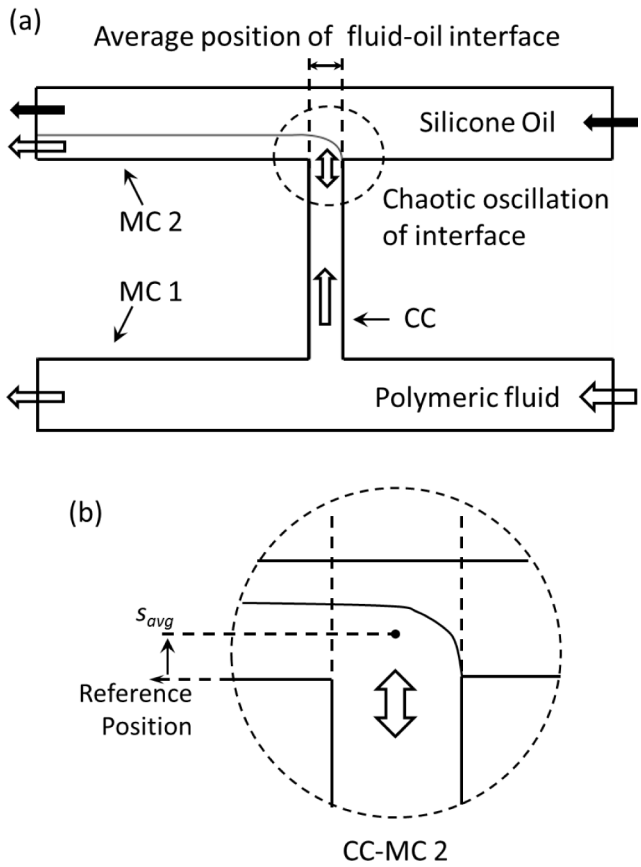

FIG. 1. (a) Viscoelastic chaotic flow generation by steady infusion of polymeric fluid and silicone oil. (b) Measurement of s_{avg} as the chaotic flow signal.

width of 100μm. All channel depths are 50 μm. The junctions between the two main channels and CC will be abbreviated as MC1-CC and CC-MC2 respectively. The micro-channel was fabricated using NOA 81 (Norland Products Inc.) ultraviolet-curable adhesive based on the method developed by Hung *et al.*[16] Briefly, a poly(dimethylsiloxane) (PDMS) mold of the micro-channel was casted from a SU-8 (MicroChem Corp.) negative mold fabricated by photolithography.[17] NOA 81 micro-channel was casted from the PDMS mold and semi-cured by ultraviolet light. Subsequently, the micro-channel was sealed by a flat semi-cured NOA 81 (with inlet ports) that was backed by a block of PDMS. The assembly was fully cured under ultraviolet light and baked in a convection oven at 80 °C for 2 hours.

Viscoelastic chaotic flow was generated by infusing a viscoelastic polymeric fluid into MC 1 at a steady flow rate, Q_{fluid}, and a Newtonian fluid (silicone oil) immiscible with the polymer solution into MC 2 at a steady flow rate Q_{oil}. Fluids were infused by syringe pumps (Legato 210p from KD Scientific Inc.). Q_{oil} was adjusted to allow the polymer solution to displace the immiscible fluid in CC and to flow into MC 2 as shown in Fig. 1(a). Q_{fluid} was increased systematically until flow instability occurred, which manifested as the fluctuation of the interface between the two fluids that were infused at steady flow rates. We measured the average position of the interface, s_{avg}, between the polymeric fluids and the immiscible fluid at the junction CC-MC2, as shown in Fig. 1(b). The measured s_{avg} were subjected to chaos analysis, in which D_2 and λ_1 were computed, for the identification of chaos and characterization of the chaotic flow.

Two polyethylene oxide (PEO) solutions that have similar elasticity (shear and extensional relaxation times) were employed. Fluid 1 (1.0 % wt/wt PEO of molecular weight $M_w = 5x10^6$ g/mol, namely PEO_1) and Fluid 2 (0.65 % wt/wt PEO of molecular weight $M_w = 8x10^6$ g/mol, namely PEO_2) were prepared to have a polymer concentration that is 15.33 times of their respective critical overlap concentrations ($c*$). $c*$ is the concentration beyond which polymer molecules in a polymer solution begin to overlap. Thus, the polymer molecules in both Fluid 1 and Fluid 2 have the same degree of overlap. For ease of preparation, Fluid 1 was chosen to be 1.0 % wt/wt PEO_1 which is equivalent to 15.33 times its c^*. Hence, Fluid 2 was prepared to 0.65 % wt/wt PEO_2 to arrive at 15.33 times its c^*. This ensures that both fluids would exhibit non-linear viscoelastic properties. The shear rheological properties of the fluids were measured using Malvern Gemini HR-Nano rotational rheometer (Malvern Instruments Ltd.), with a 4 mm cone-plate (1° cone angle) measuring system. The Maxwell relaxation time, λ_M, was computed using Equation (1).[18]

$$\lambda_M = \lim_{\omega \to 0} \frac{G'}{\omega^2 \eta_o} \tag{1}$$

where G' is storage modulus, ω angular frequency and η_o zero-shear viscosity.

The extensional relaxation time, λ_e, was measured using Haake CaBER extensional rheometer (Thermo Scientific Inc.). Fluid 1 ($\lambda_M = 1.97 \pm 0.18$ s , $\lambda_e = 121.8 \pm 8.5$ ms) and Fluid 2 ($\lambda_M = 2.14 \pm 0.11$ s, $\lambda_e = 116.2 \pm 5.1$ ms) were determined to have similar relaxation times. Both Fluid 1 and Fluid 2 contain 1 mM disodium fluorescein for visualization. The immiscible fluid employed was silicone oil with a viscosity of 50 mPa·s (Sigma-Aldrich Company). Images of the interface position between the polymeric fluids and silicone oil were captured on an epi-fluorescence inverted microscope (Nikon Ti-eclipse) by a high speed camera (Photron Fastcam SA5) at 60 frames per second. s_{avg} was measured from the captured images through image processing using MATLAB.

Fig. 2(a) shows a typical s_{avg} time evolution signal obtained from the fluctuating interface between Fluid 1 and silicone oil at $Q_{fluid} = 2.00$ ml/hr and $Q_{oil} = 0.50$ ml/hr. Fig. 3(a) shows the s_{avg} signal for Fluid 2 at $Q_{fluid} = 2.00$ ml/hr and $Q_{oil} = 0.50$ ml/hr. Both signals show that the interface fluctuated strongly over the long term, even though the flow rates remained steady. The signals were measured after 240s of setting the required Q_{fluid} and Q_{oil} to ensure that the fluctuations are not due to the transient effect of changing the flow rates. The power spectral densities (PSD) of the signals, which were computed by Fast Fourier Transform (FFT), are plotted in Fig. 2(b) and Fig. 3(b) for Fluid 1 and Fluid 2 respectively. The PSD of both Fluid 1 and Fluid 2 have a monotonic low frequency region (< 1 Hz) and decays at high frequency (> 1 Hz) which is a characteristic of a chaotic flow.[19] Nevertheless, FFT is a linear analysis; it alone is not adequate to quantify the

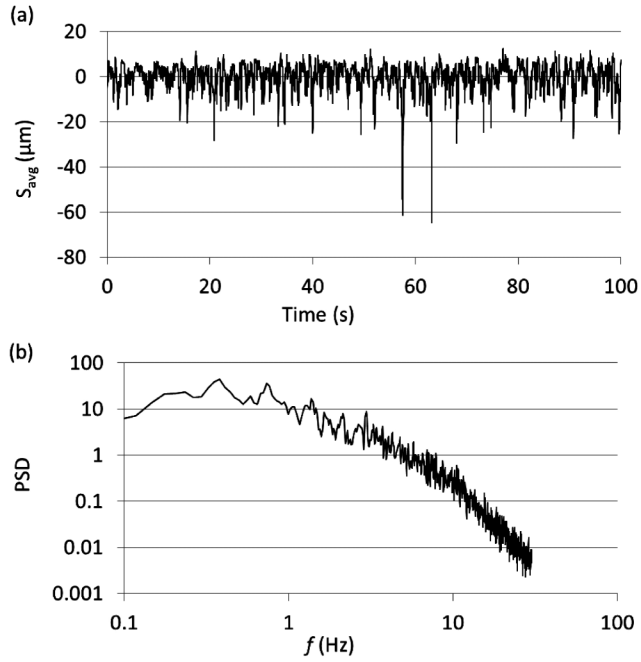

FIG. 2. (a) s_{avg} and (b) the corresponding PSD of Fluid 1 at $Q_{fluid} = 2.00$ ml/hr and $Q_{oil} = 0.50$ ml/hr.

non-linear dynamics of the chaotic flows. Therefore, chaos analysis, which is a non-linear analysis, had to be employed for further analysis and quantification of the chaotic flows.

The signals obtained were further subjected to chaos analysis to compute D_2 and λ_1 through state space reconstruction by time-delay embedding. Let a signal measured at frequency f_s be a time series $\{x_1 \quad x_2 \quad \ldots \quad x_N\}$. With a time delay of τ, an m-dimensional (m is the dimension of the state

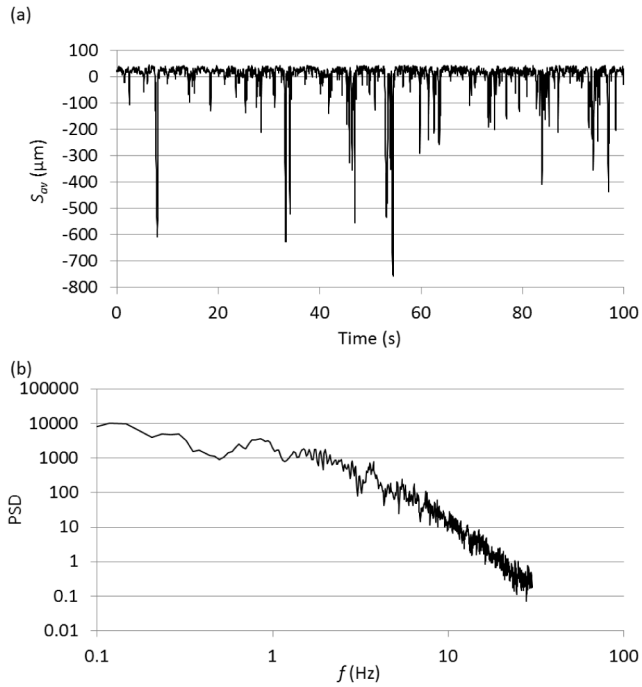

FIG. 3. (a) s_{avg} and (b) the corresponding PSD of Fluid 2 at $Q_{fluid} = 2.00$ ml/hr and $Q_{oil} = 0.50$ ml/hr.

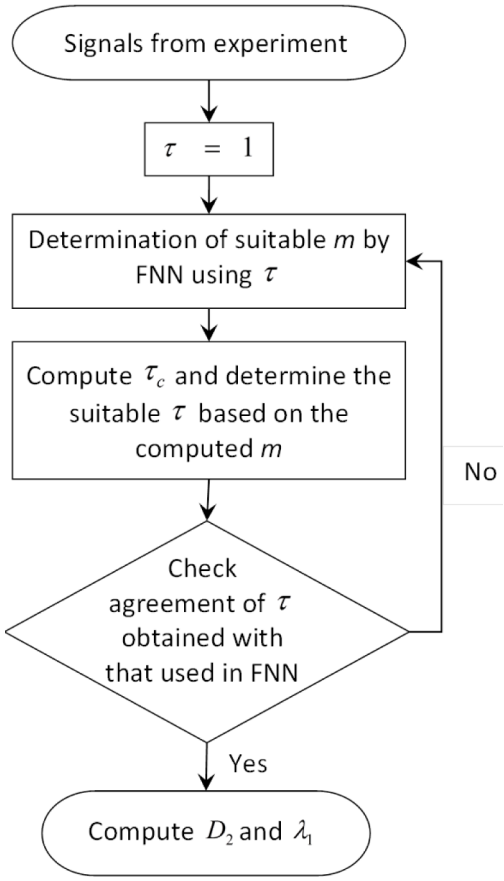

FIG. 4. Protocol for consistent selection of m and τ.

space) state space $\mathbf{X} = \begin{pmatrix} \mathbf{X}_1 & \mathbf{X}_2 & \dots & \mathbf{X}_M \end{pmatrix}^{\mathrm{T}}$ can be constructed by mapping the time series against time-lagged quantities of itself, where $\mathbf{X}_i$ is the state in the reconstructed space at time step i with $\mathbf{X_i} = \begin{pmatrix} x_i & x_{i+\tau} & \dots & x_{i+(m-1)\tau} \end{pmatrix}$. Using $\mathbf{X}$, D_2 was computed using the *Grassberger-Procaccia* algorithm[20,21] and λ_1 was computed using the algorithm proposed by Rosenstein *et al.*[22] The computation of D_2 and λ_1 requires the selection of a suitable m and τ. Based on the false nearest neighbor (FNN) method[23] and the autocorrelation time τ_c,[24] a protocol (as shown in Fig. 4) was established to enable consistent selection of these parameters across different runs of chaos analysis. m was chosen to be the smallest m that gives the fraction of FNN to be less than 0.05. The minimum permissible τ is chosen from the range of permissible τ given by Equation (2):

$$\frac{\tau_c}{m-1} \leq \tau \leq \tau_c \tag{2}$$

The fluctuating flows of Fluid 1 and Fluid 2 at $Q_{fluid} = 2.00$ ml/hr and $Q_{oil} = 0.50$ ml/hr were determined to be chaotic with their D_2 being fractional and λ_1 being positive as summarized in Table I.

TABLE I. D_2 and λ_1 of viscoelastic chaotic flows at $Q_{fluid} = 2.00$ ml/hr and $Q_{oil} = 0.50$ ml/hr in H-micro-channel.

Viscoelastic Fluid	Fluid 1	Fluid 2
m	5	5
τ	2	3
D_2	4.33	5.5
λ_1	6.25	5.16

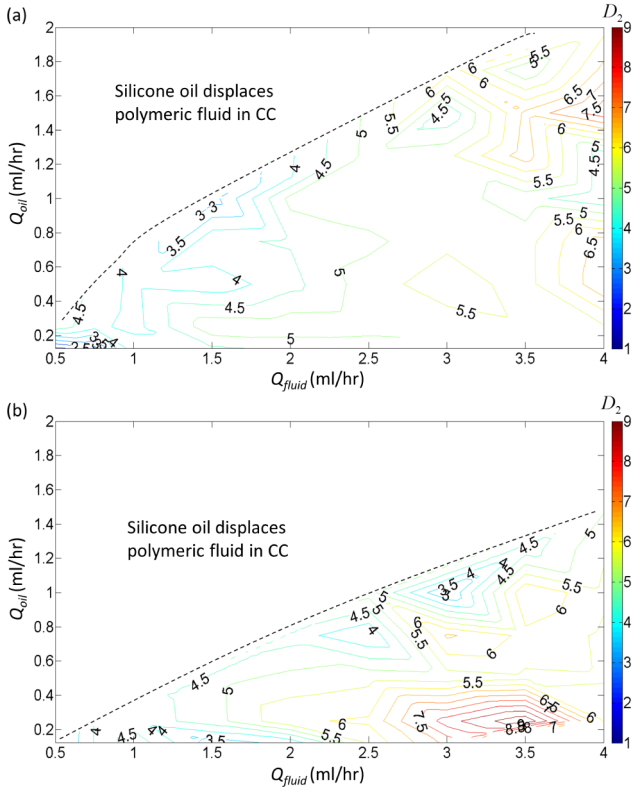

FIG. 5. D_2 characteristic map in the operating space of (a) Fluid 1 and (b) Fluid 2.

The chaotic flows of Fluid 1 and Fluid 2 for other Q_{fluid} and Q_{oil} combinations in the operating space, which are limited to 0.50ml/hr $\leq Q_{fluid} \leq$ 4.00ml/hr and 0.125ml/hr $\leq Q_{oil} \leq$ 2.00ml/hr, were analyzed similarly based on the protocol described in Fig. 4. Characteristic maps, which are two dimensional contour maps of D_2 and λ_1 plotted with Q_{fluid} and Q_{oil} being the axes, were constructed to characterize the chaotic flows generated by Fluid 1 and Fluid 2 in the operating space. The D_2 maps and λ_1 maps are plotted in Fig. 5 and Fig. 6 respectively. It was observed that the two fluids, which have similar relaxation times, have characteristic D_2 and λ_1 maps that bear similar trends but are generally distinct. From the D_2 maps, both Fluid 1 and Fluid 2 have peaks at high Q_{fluid} of beyond 3.0 ml/hr; however, the D_2 peak of Fluid 2 occurs at low Q_{oil} of 0.25 ml/hr compared to that of Fluid 1 which occur at Q_{oil} of 0.50 ml/hr and 1.50 ml/hr. In the λ_1 maps, high λ_1 occurs at high Q_{fluid} of beyond 2.5 ml/hr for both fluids; however, absent in Fluid 2, Fluid 1 exhibited a low peak at Q_{fluid} = 1.5 ml/hr and Q_{oil} = 0.75 ml/hr. The bulk viscoelastic relaxation properties (λ_M and λ_e) of Fluid 1 and Fluid 2 are similar. However, the driving force of the chaotic flows is of molecular origin and thus the differences in terms of the constituent molecules give rise to the distinct characteristic maps of the two fluids. This distinction offers a mean to differentiate between the two fluids in addition to characterizing the individual system. Furthermore, interface instability of viscoelastic fluid is the topic of relevance in many practical applications, such as mucus-air interface or biofilm stability; this analysis could potentially identify conditions for maximum instability and their correlation with molecular composition of biopolymers in each viscoelastic fluid.

In summary, chaotic flows of polymeric fluids were generated, at low Re, in a simple geometry with steady infusion of fluids driven by viscoelastic forces. The viscoelastic chaotic flows generated by two fluids, which are similar in terms of their relaxation times, were analyzed systematically with a protocol for consistent selection of m and τ across different analyses. D_2 and λ_1 of the flows showed that they are indeed chaotic with D_2 being fractional and λ_1 being positive. In addition, the D_2 and λ_1 characteristic maps of the fluids were constructed, showing the differences in the

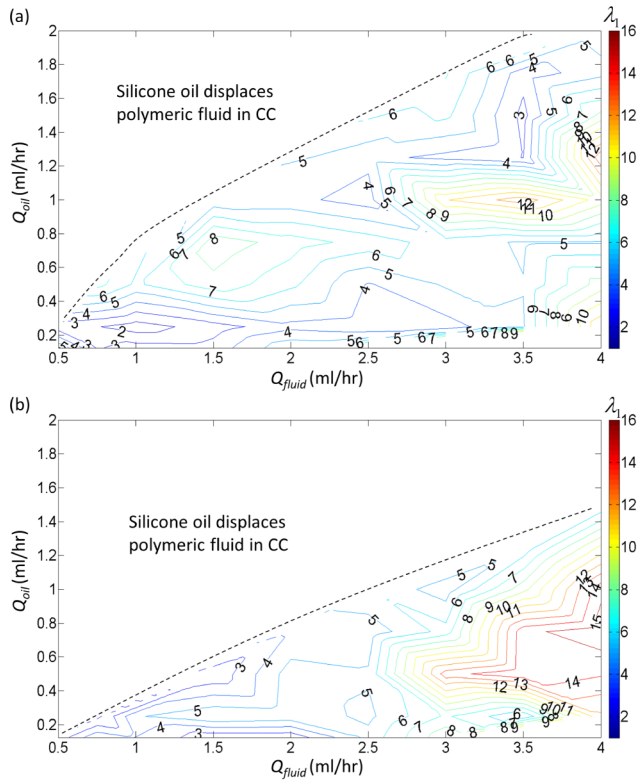

FIG. 6. λ_1 characteristic map in the operating space of (a) Fluid 1 and (b) Fluid 2.

chaotic flows generated by two similar fluids over the operating space defined by Q_{fluid} and Q_{oil}. Furthermore, the representation of the chaos parameters as characteristic maps could function as a tool to select the appropriate operating parameters to generate a desired chaotic state (instability), which is relevant in many situations involving viscoelastic fluids. This approach can be extended to the analysis of other chaotic signals such as electrocardiograms to identify abnormality through the characteristic chaos parameter maps.

ACKNOWLEDGEMENTS

This research was supported by the National Research Foundation Singapore through the Singapore MIT Alliance for Research and Technology's BioSystems and Micromechanics Inter-Disciplinary Research programme.

[1] R. J. Shilton, L. Y. Yeo, and J. R. Friend, Sensors and Actuators, B: Chemical **160**(1), 1565 (2011).
[2] X. Mao, B. K. Juluri, M. I. Lapsley, Z. S. Stratton, and T. J. Huang, Microfluidics and Nanofluidics **8**(1), 139 (2010).
[3] H. Song, M. R. Bringer, J. D. Tice, C. J. Gerdts, and R. F. Ismagilov, Applied Physics Letters **83**(22), 4664 (2003).
[4] T. Burghelea, E. Segre, I. Bar-Joseph, A. Groisman, and V. Steinberg, Physical Review E **69**(6), 066305 (2004).
[5] F.-C. Li, H. Kinoshita, X.-B. Li, M. Oishi, T. Fujii, and M. Oshima, Experimental Thermal and Fluid Science **34**(1), 20 (2010).
[6] H. Y. Gan and Y. C. Lam, AIP Advances **2**(4), (2012).
[7] J. C. Sprott, *Chaos and time-series analysis* (Oxford University Press, Oxford; New York, 2003), p. 507.
[8] J. Drahos, J. Tihon, C. Serio, and A. Lubbert, The Chemical Engineering Journal and The Biochemical Engineering Journal **64**(1), 149 (1996).
[9] S. F. Wang, R. Mosdorf, and M. Shoji, International Journal of Heat and Mass Transfer **46**(9), 1519 (2003).
[10] R. Kikuchi, T. Yano, A. Tsutsumi, K. Yoshida, M. Punchochar, and J. Drahos, Chemical Engineering Science **52**(21–22), 3741 (1997).
[11] H. M. Letzel, J. C. Schouten, R. Krishna, and C. M. van den Bleek, Chemical Engineering Science **52**(24), 4447 (1997).
[12] A. M. Guzmán and C. H. Amon, Journal of Fluid Mechanics **321**, 25 (1996).
[13] D. J. Pine, J. P. Gollub, J. F. Brady, and A. M. Leshansky, Nature **438**(7070), 997 (2005).
[14] J. I. Salisbury and Y. Sun, Annals of Biomedical Engineering **32**(10), 1348 (2004).

[15] E. W. Abdulhay, R. J. Oweis, A. M. Alhaddad, F. N. Sublaban, M. A. Radwan, and H. M. Almasaeed, Biomedical Science and Engineering **2**(3), 53 (2014).
[16] L.-H. Hung, R. Lin, and A. P. Lee, Lab on a Chip **8**(6), 983 (2008).
[17] D. C. Duffy, J. C. McDonald, O. J. A. Schueller, and G. M. Whitesides, Analytical Chemistry **70**(23), 4974 (1998).
[18] C. Tiu, G. Nicolae, and K. C. Tam, J Polym Res **3**(4), 201 (1996).
[19] F. Ravelet, A. Chiffaudel, and F. Daviaud, Journal of Fluid Mechanics **601**, 339 (2008).
[20] P. Grassberger and I. Procaccia, Physical Review Letters **50**(5), 346 (1983).
[21] P. Grassberger and I. Procaccia, Physica D: Nonlinear Phenomena **9**(1–2), 189 (1983).
[22] M. T. Rosenstein, J. J. Collins, and C. J. De Luca, Physica D: Nonlinear Phenomena **65**(1–2), 117 (1993).
[23] M. B. Kennel, R. Brown, and H. D. I. Abarbanel, Physical Review A **45**(6), 3403 (1992).
[24] J. C. Sprott, *Chaos and time-series analysis* (Oxford University Press, Oxford; New York, 2003), p. 314.